Molecular Biology of the Cell
Vol. 19, 4201–4212, October 2008

Tumor Necrosis Factor-α–elicited Stimulation of γ-Secretase Is Mediated by c-Jun N-terminal Kinase-dependent Phosphorylation of Presenilin and Nicastrin

Lan-Hsin Kuo,*† Ming-Kuan Hu,‡ Wen-Ming Hsu,§ Ying-Tsen Tung,*† Bo-Jeng Wang,* Wang-Wei Tsai,* Chen-Tung Yen,† and Yung-Feng Liao*†

*Laboratory of Molecular Neurobiology, Institute of Cellular and Organismic Biology, Academia Sinica, Taipei 115, Taiwan; †Institute of Zoology, National Taiwan University, Taipei 106, Taiwan; ‡School of Pharmacy, National Defense Medical Center, Taipei 114, Taiwan; and §Department of Surgery, National Taiwan University Hospital and National Taiwan University College of Medicine, Taipei 100, Taiwan

Submitted October 1, 2007; Revised June 24, 2008; Accepted July 23, 2008
Monitoring Editor: Erika Holzbaur

γ-Secretase is a multiprotein complex composed of presenilin (PS), nicastrin (NCT), Aph-1, and Pen-2, and it catalyzes the final proteolytic step in the processing of amyloid precursor protein to generate amyloid-β. Our previous results showed that tumor necrosis factor-α (TNF-α) can potently stimulate γ-secretase activity through a c-Jun N-terminal kinase (JNK)-dependent pathway. Here, we demonstrate that TNF-α triggers JNK-dependent serine/threonine phosphorylation of PS1 and NCT to stimulate γ-secretase activity. Blocking of JNK activity with a potent JNK inhibitor (SP600125) reduces TNF-α–triggered phosphorylation of PS1 and NCT. Consistent with this, we show that activated JNKs can be copurified with γ-secretase complexes and that active recombinant JNK2 can promote the phosphorylation of PS1 and NCT in vitro. Using site-directed mutagenesis and a synthetic peptide, we clearly show that the $Ser^{319}Thr^{320}$ motif in PS1 is an important JNK phosphorylation site that is critical for the TNF-α–elicited regulation of γ-secretase. This JNK phosphorylation of PS1 at $Ser^{319}Thr^{320}$ enhances the stability of the PS1 C-terminal fragment that is necessary for γ-secretase activity. Together, our findings strongly suggest that JNK is a critical intracellular mediator of TNF-α–elicited regulation of γ-secretase and governs the pivotal step in the assembly of functional γ-secretase.

INTRODUCTION

Extensive deposition of extracellular amyloid-β (Aβ) peptides, generated by secretase-mediated proteolysis of amyloid precursor protein (APP), is regarded as the foremost pathological hallmark of Alzheimer's disease (AD) in affected brains (Selkoe, 2001). The sequential actions of β- and γ-secretases catalyze the production of Aβ, and both proteases have been regarded as prime therapeutic targets in AD (Esler and Wolfe, 2001). Moreover, understanding the molecular mechanisms governing the enzymatic activities of these secretases should shed new light on the pathogenesis of AD.

γ-Secretase is a high-molecular-weight multimeric protein complex with aspartyl protease activity that is required for the cleavage of a wide range of type I membrane proteins, including APP and Notch receptors (Kimberly and Wolfe, 2003). The major constituents of this protease include presenilins (PS1 and PS2), nicastrin (NCT), Aph-1, and Pen-2 (Iwatsubo, 2004). Consistent with the Aβ-centered pathogenesis of AD, all the mutations in PSs that are associated with familial type AD (FAD) have been shown to favor the generation of a more amyloidogenic Aβ species, Aβ42, and lead to early onset of AD (Tanzi and Bertram, 2005). These FAD-linked PS mutations apparently affect the γ- and ε-cleavages of APP through reduced proteolytic activity of γ-secretase (Bentahir *et al.*, 2006), resulting in a decrease in total Aβ but an increase in the ratio of Aβ42/Aβ40 (De Strooper, 2007; Wolfe, 2007). In addition, these FAD-linked mutations can also lead to increased oxidative insults; it would then be possible that oxidative damage in AD could have a greater impact in the pathogenesis of this disease than Aβ does. The recently proposed alternate amyloid hypothesis, in stark contrast to the amyloid cascade hypothesis, argues that Aβ could play a neuroprotective role and that the declines in Aβ production due to FAD mutations would bleach antioxidant potential and render neurons more vulnerable to oxidative insults (Lee *et al.*, 2004, 2006). Thus, it is imperative to determine the molecular mechanism(s) governing the homeostasis of endogenous γ-secretase activity and Aβ production. These studies could then expedite the identification of novel therapeutic targets for AD.

We previously demonstrated that proinflammatory cytokines, including interferon-γ (IFN-γ), interleukin-1β (IL-1β), and tumor necrosis factor-α (TNF-α), can stimulate γ-secre-

This article was published online ahead of print in *MBC in Press* (http://www.molbiolcell.org/cgi/doi/10.1091/mbc.E07–09–0987) on July 30, 2008.

Address correspondence to: Yung-Feng Liao (yliao@sinica.edu.tw).

Abbreviations used: Aβ, amyloid-β; AD, Alzheimer's disease; AICD, amyloid precursor protein intracellular domain; APP, amyloid precursor protein; C99-CTF, 99-residue C-terminal fragment of APP; DAPT, *N*-[*N*-(3,5-difluorophenacetyl-L-alanyl)]-*S*-phenylglycine *t*-butyl ester; ELISA, enzyme-linked immunosorbent assay; JNK, c-Jun N-terminal kinase; MAP kinase, mitogen-activated protein kinase; NICD, Notch intracellular domain; PS, presenilin; TNF-α, tumor necrosis factor-α.

tase activity and Aβ production through a c-Jun N-terminal kinase (JNK)-dependent mitogen-activated protein kinase (MAPK) pathway (Liao *et al.*, 2004). Our findings thus support with a model in which extensive activation of JNK plays a pivotal role in the pathogenesis of AD (Zhu *et al.*, 2001, 2004a). Given that fibrillar Aβ can stimulate microglia to promote the release of both TNF-α and IL-1β (Combs *et al.*, 2001; Bamberger *et al.*, 2003), our data also suggest that cytokine-elicited activation of γ-secretase by the JNK pathway could constitute a positive feedback for the Aβ-induced neurotoxicity during the pathogenesis of AD.

It is clear that JNK acts as a positive regulator of γ-secretase, but the molecular mechanism underlying how JNK transduces its signal to this protease remains elusive. JNK has been shown to phosphorylate APP at Thr^{668} (Reynolds *et al.*, 2000), resulting in an enhanced APP processing by γ-secretase (Vingtdeux *et al.*, 2005). It is also possible that γ-secretase itself is subject to phosphorylation by JNK. We thus hypothesize that cytokine-elicited signaling might converge on JNK whereby γ-secretase activity can then be regulated. Here, we present direct evidence suggesting that TNF-α–elicited stimulation of γ-secretase is mediated through JNK-dependent phosphorylation of PS1 and NCT, resulting in the enhanced stability of PS1 C-terminal fragment (PS1-CTF) to facilitate the formation of functional γ-secretase complexes. These findings will pave the way for the identification of endogenous factors engaged in the regulation of γ-secretase–catalyzed proteolysis of APP.

MATERIALS AND METHODS

Reagents

BCA protein assay reagent kit, SuperSignal West Dura Extended Duration substrate, and Pico chemiluminescent substrate were purchased from Pierce (Rockford, IL). Mouse anti-JNK1 antibody was from R&D Systems (Minneapolis, MN). Rabbit anti-Notch(Val^{1744}) antibody, rabbit anti-SAPK/JNK MAPK antibody, mouse anti-phospho-SAPK/JNK antibody, and rabbit anti-JNK2 were purchased from Cell Signaling Technology (Beverly, MA). and rabbit anti-JNK3 was from Abgent (San Diego, CA). Rabbit anti-His probe (H-15) antibody, rabbit anti-GAPDH (FL-335) antibody, horseradish peroxidase (HRP)-conjugated anti-rabbit IgG, HRP-conjugated anti-rat IgG, and HRP-conjugated anti-mouse IgG were from Santa Cruz Biotechnology (Santa Cruz, CA), and Dual-Glo luciferase assay reagents, Steady-Glo luciferase assay reagents, and pRL-TK vector were from Promega (Madison, WI). Lipofectamine 2000 transfection reagent and DMEM were from Invitrogen (Carlsbad, CA). Fetal bovine serum (FBS) was from Biological Industries (Kibbutz Beit Haemek, Israel). Human Aβ40 colorimetric ELISA kit was from BioSource International (Camarillo, CA). TNF-α was from PeproTech Asia (Rehovot, Israel). HRP-conjugated anti-mouse IgG and ECL Western blotting detection reagents were from GE Healthcare (Waukesha, WI). FuGENE 6 transfection reagent, Expand long template PCR system, the Complete protease inhibitor cocktail, and the PCR nucleotide mixture were from Roche Applied Science (Indianapolis, IN). Mouse anti-phospho-Ser/Thr-Pro (MPM-2) antibody and active recombinant human JNK2 were from Upstate Biotechnology (Lake Placid, NY). Rat anti-presenilin-1 mAb, rabbit anti-APP C-terminal antibody, rabbit anti-presenilin-1-loop antibody, and mouse anti-Aβ protein (6E10) antibody were purchased from Chemicon (Temecula, CA). Rabbit anti-nicastrin was from Calbiochem (La Jolla, CA). The QuikChange site-directed mutagenesis kit was from Stratagene (La Jolla, CA). All other reagents were at least reagent grade and obtained from standard suppliers.

Cell Culture and Cell Lines

Human embryonic kidney cells (HEK293) and Chinese hamster ovary cells were maintained in DMEM supplemented with 10% FBS and 0.1 mg/ml penicillin and streptomycin. T-REx293 cells were purchased from Invitrogen and cultured in DMEM supplemented with 10% FBS and 5 μg/ml blasticidin. The generation of stably transfected cell lines, T16, T20, N7, and γ-30, was described previously (Kimberly *et al.*, 2003; Liao *et al.*, 2004; Bakshi *et al.*, 2005). HEK293-derived T16 cells were stably transfected with tetracycline-inducible Gal4/VP16-tagged full-length hAPP695 and a Gal4 promoter-driven firefly luciferase reporter gene. HEK293-derived T20 cells were stably transfected with tetracycline-inducible Gal4/VP16-tagged APP-C99 (a direct γ-secretase substrate) and a Gal4 promoter-driven firefly luciferase reporter gene. HEK293-derived N7 cells expressed mouse NΔE, a direct γ-secretase substrate. CHO-derived γ-30 cells overexpressed exogenous hPS1, hemagglutinin (HA)-tagged Aph1, and FLAG-tagged Pen-2. CHO-derived γNCT-36 cells overexpressed exogenous hPS1, His-tagged NCT, HA-tagged Aph1, and FLAG-tagged Pen-2. Cells were incubated in a humidified incubator at 37°C in 5% CO_2.

Transient Transfection of Mammalian Cells

Transfection of HEK293, T20, γ-30, and γNCT-36 cells was performed using FuGENE 6 transfection reagent or Lipofectamine 2000 transfection reagent as described by the manufacturers. Cells were plated onto six-well microplates or 10-cm plates and grown to ~60–80% confluency before transfection. On the day of transfection, the culture medium was replaced with fresh 2 ml/well or 10 ml/plate of DMEM supplemented with 10% FBS. DNA constructs (1 μg) and pRL-TK (0.1 μg) were diluted in 100 μl of serum-free DMEM and mixed with 3 μl of FuGENE 6 or Lipofectamine 2000, followed by incubation at room temperature for 15 min. Transfection mixtures were added dropwise into cell culture medium and incubated at 37°C for 24 h. Transfected cells were harvested by PBS containing 20 mM EDTA and lysed with 1× passive lysis buffer (PLB, Promega, Madison, WI) or CHAPSO lysis buffer (50 mM Tris-HCl, pH 8.0, 1% CHAPSO, 150 mM NaCl, 25 mM β-glycerophosphate, 1 mM Na_3VO_4, and the Complete protease inhibitor cocktail). Clarified lysates were subject to luciferase assay using the Dual-Glo luciferase assay reagent kit for the measurement of γ-secretase activity or affinity pulldown using HIS-Select Cobalt Affinity Gel (Sigma, St. Louis, MO) for the isolation of γ-secretase complexes. Protein content of lysates was determined by the BCA protein assay reagent kit.

Transfection of Small Interfering RNAs Targeting JNK1, JNK2, and JNK3

Small interfering RNA (siRNA) duplex oligoribonucleotides against human JNK1 (si-JNK1), JNK2 (si-JNK2), and JNK3 (si-JNK3) were chemically synthesized by Invitrogen. The target sequences for si-JNK1 were 5′-GGA GCU CAA GGA AUA GUA U-3′ (sense strand) and 5′-AUA CUA UUC CUU GAG CUC C-3′ (antisense strand); for si-JNK2, 5′-GCU CUG CGU CAC CCA UAC A-3′ (sense strand) and 5′-UGU AUG GGU GAC GCA GAG C-3′ (antisense strand); and for si-JNK3, 5′-GGG AUU UAA AAC CAA GUA A-3′ (sense strand) and 5′-UUA CUU GGU UUU AAA UCC C-3′ (antisense strand). The human GAPDH siRNAs and nonspecific scrambled siRNAs were from Ambion (Austin, TX). Gene-targeting siRNA oligos (100 pmol; for individual knockdown of JNK1, JNK2, or JNK3) were mixed with nonspecific scramble siRNAs (100 pmol) and transfected into T20 cells by using the Lipofectamine 2000 transfection reagent (Invitrogen) according to the manufacturer's instructions. Additionally, two gene-targeting siRNA oligos (100 pmol each; for combinatorial knockdown of JNK1+JNK2, JNK1+JNK3, or JNK2+JNK3) were mixed and transfected into T20 cells. T20 cells (2.5×10^4/well) were plated in 12-well microplates and transfected with siRNAs for 24 h, followed by an additional incubation with culture medium containing 1 μg/ml tetracycline in the presence or absence of TNF-α (50 ng/ml) at 37°C for 9 h. Clarified lysates of transfected cells were prepared and analyzed by Steady-Glo luciferase assay reagents to determine γ-secretase activity, and conditioned media were analyzed by the colorimetric Aβ40 ELISA kit to measure secreted Aβ40. Protein contents of cell lysates were determined by BCA protein assay reagent kit. A nonspecific oligonucleotide (Silencer Negative Control 1, catalogue no. AM4611, Ambion) that is not homologous to any known genes was used as a negative control to rule out nonspecific cellular events caused by the introduction of the siRNAs into cells. The transcript levels of JNKs in transfected cells were quantitated by real-time PCR with isoform-specific primer pairs to determine the knockdown efficiency of respective siRNAs.

Real-Time PCR to Quantitate the RNA Transcripts of JNK Isoforms

Total RNA of transfected cells was prepared by using TRIzol (Invitrogen) and was used to generate the first strand cDNA by SuperScript III First-strand cDNA Synthesis Kit (Invitrogen). Equivalent amounts of cDNA were used in quantitative PCR on DNA Engine Opticon Real-Time PCR Detection System (Bio-Rad, Hercules, CA) with following isoform-specific primer pairs: For JNK1, forward primer: 5′-GTTTGCCACAAAATCCTC-3′, reverse primer: 5′-CTGAGAGCCATTGATCAC-3′; for JNK2, forward primer: 5′-TGAAACTTGCCCACCCTT-3′, reverse primer: 5′-CCTTGGAATATCACACAACCTTTC-3′; and for JNK3, forward primer: 5′-CCAACATTGGATGTGAAAATTGCCT-3′, reverse primer: 5′-GGTACGCTCTCTTGGCATGT-3′ (Katagiri *et al.*, 2006). The levels of human GAPDH transcripts (forward primer: 5′-GTGGTCTCCTCTGACTTCAAC-3′ and reverse primer: 5′-TCTCTTCCTCTTGTGCTCTTG-3′) were determined as an internal control. Cycling conditions were 95°C for 3 min, followed by 40 cycles of 94°C for 30 s, 55°C for 30 s, and 72°C for 1 min. For quantitation, the transcript levels of JNK isoforms were individually normalized to those of GAPDH. The data were expressed as the average (±SD) of triplicate measurements from three independent experiments.

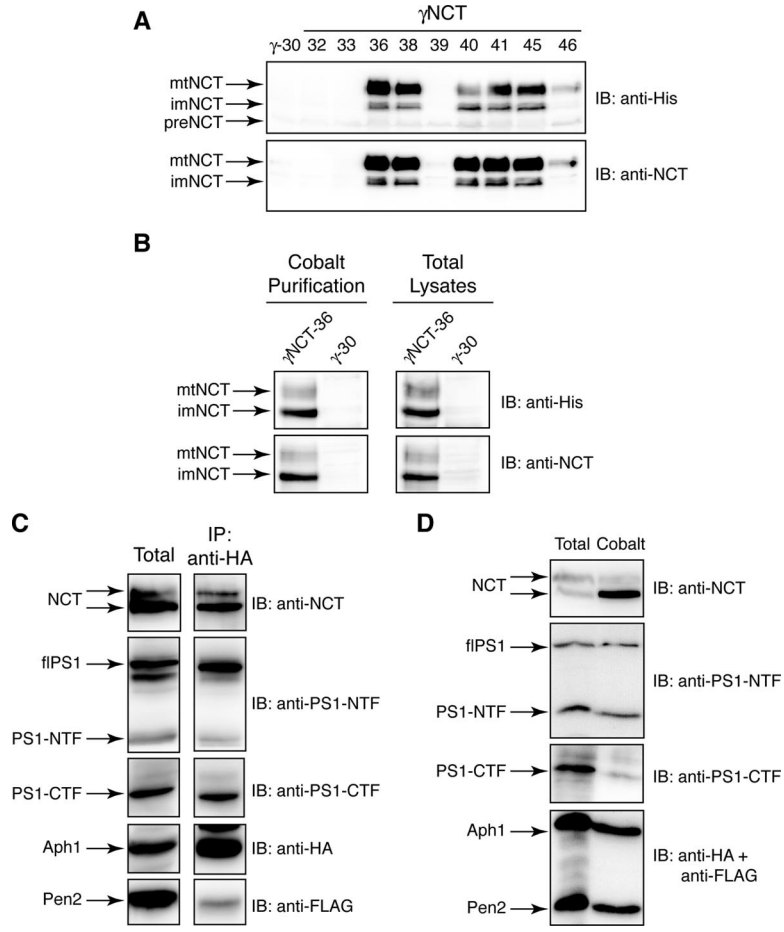

Figure 1. Generation of a cell line stably overexpressing His-tagged NCT. Cells of the parental clone γ-30 that overexpress human PS1, FLAG-tagged Pen-2, HA-tagged Aph1α2, and APP were transfected with pcDNA6-NCT-V5-His (His-NCT). Transfected cells were cultured in DMEM supplemented with 10% FBS, 200 μg/ml hygromycin, 250 μg/ml, zeocin, 2.5 μg/ml puromycin, 200 μg/ml geneticin (G418), and 5 μg/ml blasticidin (DMEM-HZPGB). (A) Each of the independent clones was isolated and screened for the expression of His-tagged NCT by Western blotting as described in *Materials and Methods.* Clarified lysates prepared from individual clones with equivalent amounts of protein were resolved by SDS-PAGE and analyzed by Western blotting with anti-His (top panel) and anti-NCT (bottom panel) antibodies. Clone numbers are denoted at the top of the blots. The optimal cell line was the one exhibiting the highest amount of mature NCT (mtNCT). Based on this criterion, clone 36 (γNCT-36) was selected as the cellular model for future experiments. (B) Clarified lysates of γ-30 and γNCT-36 cells were processed through HIS-Select Cobalt Affinity Gel, and affinity-purified proteins were resolved by SDS-PAGE and analyzed by Western blotting using rabbit anti-His antibody (top panel) and rabbit anti-NCT antibody (bottom panel). Both the His-tagged mtNCT and immature NCT (imNCT) in γNCT-36 cells, but not the endogenous NCT in the parental γ-30 cells, can be efficiently pulled down by HIS-Select Cobalt matrix through affinity with the His tag of the recombinant NCT. (C) Clarified lysates of γNCT-36 cells were coimmunoprecipitated by an anti-HA antibody, and precipitated proteins were resolved by SDS-PAGE and analyzed by Western blotting to visualize NCT, PS1 (flPS1, PS1-NTF, and PS1-CTF), Aph1, and Pen-2 with specific antibodies. (D) Clarified lysates of γNCT-36 cells were processed through HIS-Select Cobalt Affinity Gel, and affinity-purified proteins were resolved by SDS-PAGE and analyzed by Western blotting to visualize NCT, PS1 (flPS1, PS1-NTF, and PS1-CTF), Aph1, and Pen-2 with specific antibodies. Blots shown in C and D prove successful isolation of the active γ-secretase complexes, but do not necessarily reflect the actual stoichiometry of the enzyme components.

Generation of a Stably Transfected Cell Line γNCT-36

The parental cell line γ-30 and nicastrin expression vector were gifts kindly provided by Dr. Michael Wolfe (Brigham and Women's Hospital and Harvard Medical School, Boston, MA), and the generation of CHO-derived γ-30 cells was previously described (Kimberly *et al.*, 2003). On the day of transfection, γ-30 cells on a 10-cm dish with ~50% confluency were transfected with 5 μg of pcDNA6-Nicastrin-V5-His (NCT-His) by FuGENE 6 transfection reagent according to the manufacturer's instructions. Transfected cells were cultured in DMEM supplemented with 10% FBS, 250 μg/ml hygromycin, 250 μg/ml zeocin, 2.5 μg/ml puromycin, 200 μg/ml geneticin (G418), and 5 μg/ml blasticidin (DMEM-HZPGB), and single colonies resistant to antibiotic selection were isolated individually using cloning cylinders. Each of the independent cell lines was screened for the overexpression of His-tagged NCT. Individually isolated cell lines were plated into 12-well microplates in DMEM-HZPGB for 24 h. Cells were lysed in CHAPSO lysis buffer, and His-tagged NCT along with other γ-secretase components was pulled down by HIS-Selected Cobalt Affinity Gel (Sigma). The affinity-purified proteins were resolved by SDS-PAGE and analyzed by Western blotting using rabbit anti-His antibody and rabbit anti-NCT antibody. The optimal cell line was the one exhibiting the highest amount of mature NCT. Based on this criterion, clone γNCT-36 was selected for future experiments (Figure 1).

TNF-α–elicited Phosphorylation of NCT and PSI-1

On the day of the experiment, γNCT-36 cells (10^7 cells/plates) in 10-cm culture dishes were preincubated with DMEM containing 0.5% FBS at 37°C for 3 h, followed by the addition of TNF-α to a final concentration of 50 ng/ml and incubation at 37°C for various intervals. For the treatment with JNK inhibitor, γNCT-36 cells were pretreated with SP600125 (10 μM) or DMSO (1%) for 30 min, followed by the addition of TNF-α (50 ng/ml) and incubation at 37°C for 1.5 h. Cells were harvested and lysed in a CHAPSO (1%)-containing buffer. Intact γ-secretase complexes derived from clarified lysates of treated and untreated γNCT-36 cells were purified by HIS-Selected Cobalt Affinity Gel (Sigma) through their affinity with His-tagged NCT. Affinity-purified proteins were resolved by SDS-PAGE and analyzed by Western blotting with anti-phospho-serine/threonine antibody to determine the phosphorylation of immature and mature NCT (~130 and 180 kDa) and full-length PS1 (~50 kDa). The same blots were stripped and reprobed with anti-NCT and anti-PS1-NTF antibodies, respectively, to determine the levels of total NCT and PS1.

Cell-based γ-Secretase Assays

The quantitative measurement of γ-secretase activity using T20 cells has been previously described (Liao *et al.*, 2004, 2007). To examine TNF-α–elicited effects on γ-secretase, T20 cells stably transfected with C99-GV and Gal4-Luc were trypsinized and plated onto six-well microplates at 5×10^5 cells/well with 1 ml/well serum-free DMEM. After incubation at 37°C overnight, cells were treated with 50 ng/ml TNF-α in DMEM containing 1 μg/ml tetracycline and incubated at 37°C for various intervals as specified. Cells incubated with serum-free DMEM containing 1 μg/ml tetracycline alone were used to define the basal level of γ-secretase activity at each time point. To terminate the reactions, cells were harvested with PBS containing 20 mM EDTA and dissolved in 100 μl of 1× PLB. After the removal of cell debris by centrifugation, the activity of expressed luciferase reporter gene in clarified lysates was determined by mixing 20 μl of lysates and 20 μl of Steady-Glo luciferase assay reagent in a 96-well LumiNunc microplate (Nunc, Naperville, IL). Luminescence in individual microwells was determined by a VictorLight microplate luminometer (PerkinElmer, Waltham, MA) and subsequently normalized by the protein content of the corresponding lysates. The protein concentrations of clarified lysates were determined by the BCA protein assay kit as described in manufacturer's instructions. The normalized luciferase signal emitted by T20 cells in serum-free DMEM without tetracycline was referred to as onefold of activation. For treatments with chemical compounds, such as compound E,

DAPT, MAP kinase inhibitors, compounds were added into the medium to a final concentration of 10 μM or as specified, and the reactions were incubated at 37°C for various intervals as specified.

SDS-PAGE and Western Blot Analysis

Clarified cell lysates containing equivalent amounts of proteins were mixed with equal volumes of 2× SDS sample buffer (125 mM Tris-HCl, pH 6.8, 4% SDS, 20% glycerol, 2% dithiothreitol, and 5% β-mercaptoethanol) and boiled at 100°C for 5 min. Denatured proteins were resolved in Tris glycine polyacrylamide gels (10 or 12%) and transferred electrophoretically to polyvinylidene difluoride membranes (Pall Corporation, East Hills, NY). Unbound areas on the membranes were blocked by a blocking buffer [3% BSA, 0.1% Tween-20 in TBS (TBST)] at room temperature for 1 h, followed by a brief rinse with TBST. Blocked membranes were probed with appropriate dilutions of primary antibody in the blocking buffer at room temperature for 1 h. After extensive washes with TBST to remove unbound primary antibody, washed membranes were incubated with appropriate HRP-conjugated secondary antibody in TBST at room temperature for 1 h. After the removal of unbound secondary antibody, antibody-reacted proteins were visualized by chemiluminescence using the SuperSignal West Femto or Dura reagents. Images were captured by and processed with ChemiGenius2 (Syngene, Frederick, MD). The antibodies used and their dilutions were as follows: anti-phospho-JNK and anti-JNK (Cell Signaling Technology, Beverly, MA), 1:1000; anti-phospho-Ser/Thr (MPM-2), 1:4000; anti-PS1-NTF (N-19), 1:4000; anti-nicastrin, 1:4000; anti-Aβ (6E10), 1:1000; anti-APP-CTF, 1:4000; anti-GAPDH, 1:4000; HRP-conjugated anti-mouse IgG (Amersham Biosciences, Piscataway, NJ) 1:10,000; and HRP-conjugated anti-rabbit IgG (Santa Cruz), 1:1000.

Site-directed Mutagenesis of Human PS1

The expression vector encoding the full-length human wild-type PS1 (pcDNA3.1-PS1) was kindly provided by Dr. Michael Wolfe (Brigham and Women's Hospital and Harvard Medical School, Boston, MA; Kimberly *et al.*, 2003). To generate a human PS1 mutant (PS1-S319AT320A) that lacks a putative phosphorylation site, adjacent serine and threonine ($S^{319}T^{320}$) in PS1 predicted to be susceptible to phosphorylation (http://www.cbs.dtu.dk/services/NetPhos/; the algorithm of this analysis can be found in Blom *et al.*, 1999) were both replaced with alanines using the QuikChange site-directed mutagenesis kit according to the manufacturer's instructions. Two complementary oligonucleotides containing the desired mutations, flanked by unmodified nucleotide sequences, were synthesized. The paired primers for the generation of mutant PS1-S319AT320A were S319AT320A-forward (5′-AAG TAT AAT GCA GAA GCC GCA GAA AGG GAG TCA CAA-3′) and S319AT320A-reverse (5′-AGC TCG TGA CTC AGG TGC AGC GCG ATG AGG CCC TAG-3′). The underlined nucleotides denote the base changes made to incorporate the desired missense mutations. The mutagenized sequences were confirmed by DNA sequencing.

Microsomal Preparation of γ-Secretase

The microsomal preparation and solubilization of γ-secretase from γ-30 and γNCT-36 cells were performed as previously described (Fraering *et al.*, 2004). A total of 10^8 γNCT-36 cells was harvested and resuspended in 10 ml of MES buffer (50 mM MES, pH 6.0, 150 mM NaCl, 5 mM $MgCl_2$, 5 mM $CaCl_2$, and the Complete protease inhibitor cocktail). The cells were lysed by being processed through a French Press (Thermo Fisher Scientific, Waltham, MA) once at 1500 psi. Nuclei and cellular debris were removed by centrifugation at 1500 *g* for 10 min, and the postnuclear supernatant was saved and centrifuged at 100,000× *g* for 1 h at 4°C to pellet the total membranes (to yield the membrane preparation). Membrane pellets were resuspended in 2 ml of ice-cold MES buffer (0.1 M $NaHCO_3$, pH 11.3) and were then repelleted at 100,000× *g* for 1 h at 4°C to obtain the total microsomal membranes.

In Vitro Kinase Assay

JNK-dependent phosphorylation of γ-secretase components was carried out as described previously (Wei *et al.*, 1999). In brief, the total microsomal membranes prepared from 10^8 γNCT-36 cells were resuspended in 0.6 ml of solubilization buffer (1% digitonin, 25 mM HEPES, pH 7.5, 150 mM NaCl, 5 mM $MgCl_2$, 5 mM $CaCl_2$, and the Complete protease inhibitor cocktail) and incubated at 4°C for 1 h, followed by centrifugation at 16,100×*g* for 10 min at 4°C to remove insoluble materials. γ-Secretase complexes in the solubilized supernatant was isolated by HIS-Select Cobalt Affinity Gel (Sigma, 150 μl of 50% suspension) through the affinity with His-tagged NCT and eluted by the elution buffer (50 mM sodium phosphate, pH 8.0, 0.3 M sodium chloride, 250 mM imidazole). Eluates of equivalent volume containing the affinity-precipitated γ-secretase complexes were then incubated with 0.2 μg of active JNK2 (Upstate) and 200 μM ATP in kinase reaction buffer in the presence or absence of SP600125 (20 μM) for 1.5 h at 30°C. Kinase reactions were terminated by the addition of SDS sample buffer. Proteins were resolved by 10–12% SDS-PAGE, and phosphorylated γ-secretase components were detected by Western blotting with anti-phospho-Ser/Thr antibodies. Duplicate blots were probed with anti-JNK2, anti-PS1, and anti-NCT antibodies for the identification of phosphorylated proteins.

To assess the JNK phosphorylation motif of PS1, synthetic peptide containing either the wild-type Ser^{319}-Thr^{320} motif (ST; NH_2-KYNAE**ST**ERESQ-COOH) or an altered motif substituting both Ser^{319} and Thr^{320} residues with alanines (AA; NH_2-KYNAE**AA**ERESQ-COOH) were synthesized by Genesis Biotech (Taipei, Taiwan) and were used as competitors of in vitro JNK phosphorylation of PS1 as described above. Boldface letters denote the critical amino acids essential for JNK phosphorylation in wild-type PS1 and those substituted by alanines in mutant peptide.

Cell-Free γ-Secretase Assay

To determine the microsomal γ-secretase activity in response to JNK phosphorylation, we used a robust in vitro cell-free assay to assess the microsomal membrane-associated γ-secretase activity (McLendon *et al.*, 2000; Qin *et al.*, 2003; Weggen *et al.*, 2003). Briefly, the total microsomal membranes derived from γNCT-36 or T20 cells were resuspended in 0.5 ml of kinase reaction buffer (25 mM Tris, pH 7.5, 5 mM β-glycerolphosphate, 2 mM 2-mercaptoethanol, 0.1 mM Na_3VO_4, 10 mM $MgCl_2$, Complete protease inhibitor cocktail, and 0.02 mM EDTA). An aliquot of resuspended membrane (38 μl) was incubated with 0.2 μg of active JNK2 (Upstate) and 200 μM ATP (to a final volume of 40 μl) for 2 h at 37 or 4°C. Isolated γ-secretase has been previously shown to exhibit a pH optimum at pH 7.5 and be able to cleave solubilized APP-CTFs in cell-free conditions (Esler *et al.*, 2002; Fraering *et al.*, 2004). Reactions lacking JNK2 were included as controls. Kinase reactions were terminated by the addition of SDS sample buffer and boiling at 100°C for 10 min. Proteins were resolved by tricine (16.5%) SDS-PAGE, and the levels of C99, C83, and AICD were visualized by Western blotting using anti-Aβ1–17 (clone 6E10, for C99) and anti-APP C-terminus (for C83 and AICD) antibodies, respectively.

Quantitative Densitometry and Statistical Analysis

Quantitative analysis of Western blots was conducted with the TotalLab v2.01 program by determining the relative density of the immunoreactive bands after acquisition of the blot image with ChemiGenius2 (Syngene). Phosphorylation levels were defined as the ratio of phospho-protein to total protein. Results were expressed as the mean (±SD) of triplicate measurements from a representative experiment. Statistical analyses were done by a one-tailed Student's *t* test, and $p < 0.05$ was considered significant.

RESULTS

TNF-α Enhances the Phosphorylation of PS1 and NCT

We previously showed that TNF-α can activate γ-secretase through a JNK-dependent MAPK pathway. Therefore, we sought to determine whether this TNF-α–elicited regulation of γ-secretase is due to JNK-dependent phosphorylation of this protease. To improve the efficiency of isolation of intact γ-secretase complexes, we generated a CHO-derived cell line (γNCT-36) from parental γ-30 cells that constitutively coexpresses a His-tagged NCT along with human wild-type PS1, HA-tagged Aph-1α2, FLAG-tagged Pen-2, and APP (Kimberly *et al.*, 2003). Overexpression of His-tagged NCT in γNCT-36 cells was verified by the pulldown of recombinant NCT using the HIS-Select Affinity Gel chromatography (Figure 1B). Nonglycosylated NCT, immature NCT, and mature NCT were all detected in this cell line, indicating that the maturation of recombinant NCT is not affected by the C-terminal 6XHis tag. We then demonstrated that functional γ-secretase complexes could be formed in γNCT-36 cells, as evidenced by the successful isolation of all four constituents (PS1 heterodimers, NCT, Aph-1, and Pen-2) using coimmunoprecipitation with an anti-HA antibody (reactive with the HA-tagged Aph-1) and HIS-Select Cobalt Affinity Gel (Figure 1, C and D).

To examine the TNF-α–elicited phosphorylation of γ-secretase, γNCT-36 cells were treated with TNF-α for various intervals. We found that the level of phosphorylation of full-length PS1 (flPS1) in TNF-α–treated γNCT-36 cells was dramatically increased at 30 min, peaked at 1.5 h, and then returned to the basal level at 2.5 h (Figure 2B, top panel). Consistent with this profile, the phosphorylation level of mature NCT in TNF-α–treated cells was significantly increased at 1.5 h and was sustained for up to 2.5 h (Figure 2A, top panel). The total protein levels of NCT and flPS1

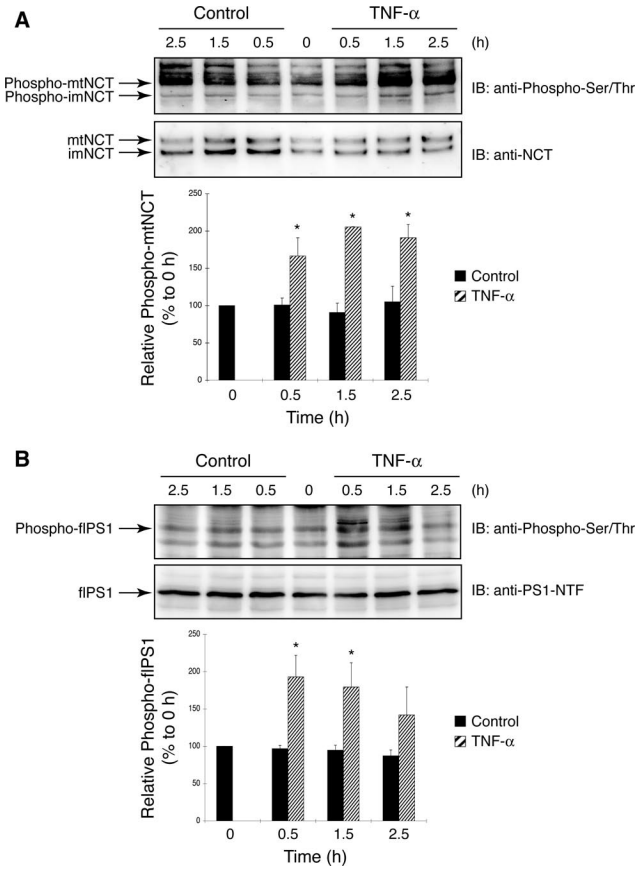

Figure 2. TNF-α enhances the phosphorylation of NCT and PS1. γNCT-36 cells (10^7 cells/plates) in 10-cm culture dishes were preincubated with DMEM containing 0.5% FBS at 37°C for 3 h, followed by the addition of TNF-α to a final concentration of 50 ng/ml and incubation at 37°C for various intervals. Intact γ-secretase complexes were purified by HIS-Selected Cobalt Affinity Gel chromatography through the His-tagged NCT. Affinity-purified proteins were resolved by SDS-PAGE and analyzed by Western blotting with anti-phospho-serine/threonine antibody to determine the phosphorylation of mature and immature NCT (phospho-mtNCT and phospho-imNCT, top panel, A) and full-length PS1 (phospho-flPS1, top panel, B). After stripping, the top and lower halves of the blot were reprobed with anti-NCT and anti-PS1-NTF antibodies, respectively, to determine the levels of total NCT (mtNCT and imNCT, bottom panel, A) and PS1 (flPS1, bottom panel, B). Quantitative data are expressed as the mean (±SD) from three independent experiments and analyzed by Student's *t* test. *$p < 0.05$ denotes versus control at the same time. mtNCT, mature NCT; imNCT, immature NCT; flPS1, full-length PS1. Alteration in phosphorylation of mtNCT was noted in the control samples of 2.5 h, but could not be consistently observed.

remained unaffected (Figure 2A, bottom panel, and B, bottom panel).

Down-Regulation of JNKs Attenuates Endogenous and TNF-α–elicited γ-Secretase Activity

To verify that the TNF-α–elicited stimulation of γ-secretase activity is mediated through a JNK-dependent pathway, we used an RNA interference (RNAi) approach to determine whether specific down-regulation of JNK isoforms is sufficient to block TNF-α–elicited stimulation of γ-secretase. Isoform-specific siRNA oligonucleotides targeting JNK1, JNK2, and JNK3 (si-JNK1, si-JNK2, and si-JNK3) were transfected individually or combinatorially into T20 cells and were shown to significantly down-regulate the expression of the targeted JNK isoform(s) (Figure 3B). The knockdown efficiency of these isoform-specific siRNAs ranged from 40 to 80% as estimated by real-time PCR. We found that TNF-α–elicited stimulation of γ-secretase was significantly attenuated by the down-regulation of selective JNKs and was completely abolished by the combined down-regulation of JNK1 and JNK2, whereas γ-secretase activity in mock-transfected cells was elevated ~100% by the stimulation of TNF-α (Figure 3A). In the absence of TNF-α, the down-regulation of JNKs also resulted in a significant reduction in endogenous basal γ-secretase activity, suggesting that JNKs might govern the function of this protease. Consistently, the levels of secreted Aβ40 from cells that are transfected with JNK-targeting siRNAs were significantly reduced (Figure 3C). The attenuation of γ-secretase activity through the down-regulation of JNK, reminiscent of the effect of the JNK antagonist SP600125 (Liao *et al.*, 2004), is consistent with the model that JNKs play a critical role in maintaining the homeostasis of endogenous γ-secretase activity.

Inhibition of JNK Significantly Attenuates TNF-α–elicited Phosphorylation of NCT and PS1

To further verify the critical role of JNKs in TNF-α–elicited phosphorylation of PS1 and NCT, γNCT-36 cells were pretreated with SP600125, a specific JNK inhibitor, in the presence of TNF-α. We found that the TNF-α–induced phosphorylation of both NCT and full-length PS1 was suppressed by SP600125 down to the basal level while the total protein levels of NCT and flPS1 were unchanged (Figure 4). Active JNK was copurified with γ-secretase complexes, suggesting that, in the presence or absence of extracellular stimuli, JNK can intimately associate with γ-secretase in a cellular environment (Figure 4A). Together, these findings strongly suggest that JNK is a crucial mediator of TNF-α–elicited stimulation of γ-secretase.

JNK Can Directly Interact with γ-Secretase and Promote the Phosphorylation of NCT and PS1

To determine whether γ-secretase can be directly phosphorylated by JNK, we used an in vitro kinase assay in which purified active JNK2 could directly interact with intact γ-secretase complexes isolated from the microsomal membranes of γNCT-36 cells. Solubilized γ-secretase purified by HIS-Select Cobalt Affinity Gel chromatography was incubated with active JNK2 recombinant protein with or without SP600125 at 30°C for 1 h. Consistent with our results obtained from cell-based assays, we found that active JNK2 can directly phosphorylate NCT and PS1 in vitro, inducing ~127 and 77% increases in the levels of phosphorylation of NCT and flPS1, respectively (Figure 5). This JNK2-induced phosphorylation of γ-secretase can be completely abolished by SP600125 that can also suppress the autophosphorylation of JNK (Figure 5B). The total levels of NCT, JNK2, and flPS1 indicate consistent protein loading in these in vitro kinase assays (Figure 5A). Given that JNKs can also copurify with γ-secretase complexes, it is plausible that JNKs can physically interact with and modify this protease to promote its enzymatic activity.

Active JNK2 Promotes γ-Secretase–catalyzed Processing of APP-C99 and APP-C83 to Enhance the Production of AICD

To further substantiate that JNK-dependent phosphorylation of γ-secretase could affect its proteolytic activity, solubilized membrane preparation of γNCT-36 containing

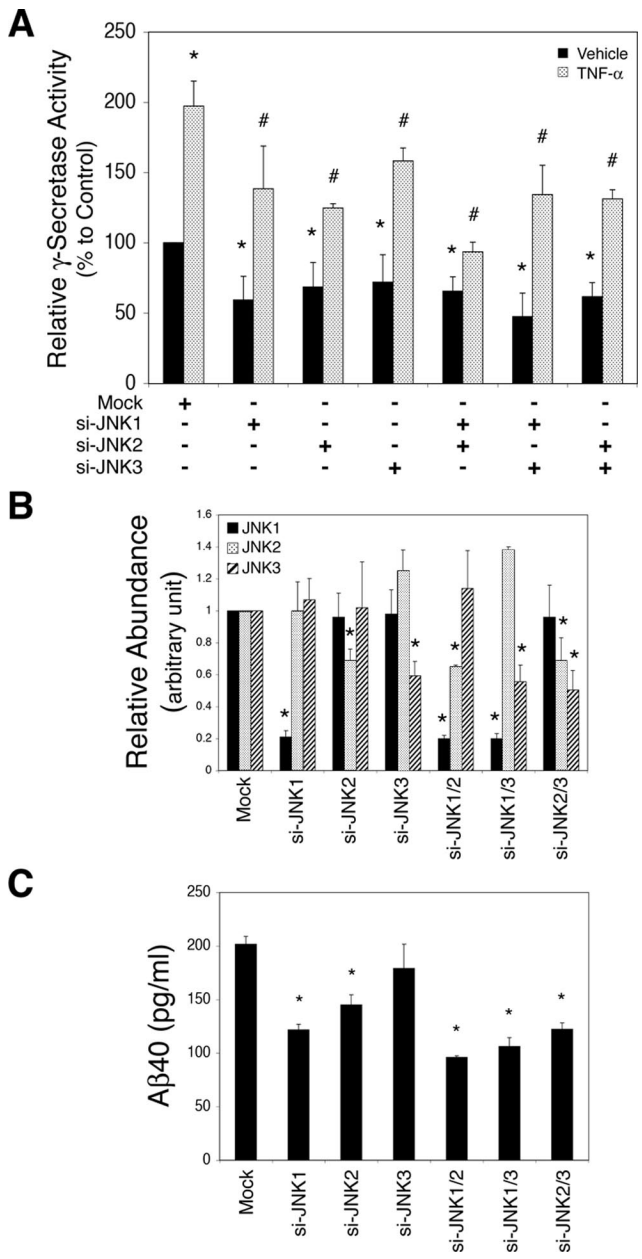

Figure 3. Down-regulation of JNKs attenuates TNF-α–elicited stimulation of γ-secretase activity. (A) T20 cells were individually transfected with siRNA-JNK1 (si-JNK1), siRNA-JNK2 (si-JNK2), or siRNA-JNK3 (si-JNK3; 100 pmol) along with a nonspecific siRNA (100 pmol) as described in *Materials and Methods.* Additionally, T20 cells were also transfected with the combination of si-JNK1+si-JNK2, si-JNK1+si-JNK3, or si-JNK2+si-JNK3 (100 pmol each). Transfected cells were incubated with culture medium containing 1 μg/ml tetracycline in the presence (solid bar) or absence (open bar) of TNF-α (50 ng/ml) at 37°C for 12 h. γ-Secretase activity in clarified lysates of transfected cells was determined by using Dual-Glo luciferase assay reagents and compared with that of cells transfected with a nonspecific siRNA (Mock), which is referred to as 100% of the relative γ-secretase activity. Results are expressed as the mean (±SD) from four independent experiments and analyzed by Student's *t* test. *$p < 0.05$ versus nonstimulated Mock. #$p < 0.05$ versus stimulated Mock. (B) The siRNAi-induced down-regulation of JNK1, JNK2, and JNK3 was determined by real-time PCR with specific primer pairs targeting JNK1 (solid bar), JNK2 (hatched bar), and JNK3 (striped bar), respectively. The abundance of GAPDH were also determined as a internal control. Relative abundance was determined by normalizing the transcript level of individual JNK isoform with that of GAPDH. Quantitative data are expressed as the mean (±SD) from three independent experiments and analyzed by Student's *t* test. *$p < 0.05$ versus Mock. (C) Secreted Aβ40 in the conditioned media of T20 cells transfected with siRNAs was quantitated by an Aβ40 sandwich ELISA kit. Basal levels of Aβ production in cells transfected with a nonspecific siRNA (Mock) were also determined. Data are shown as the mean ± SD of triplicate measurements from a representative experiment analyzed by Student's *t* test. *$p < 0.05$ versus Mock.

γ-secretase and APP was incubated with active JNK2 recombinant protein at 30 or 4°C. Our data showed that, in the presence of active JNK2, γ-secretase–mediated processing of the APP C-terminal fragments, APP-C99 and APP-C83, is significantly enhanced, evidenced by the diminished accumulation of C99 and C83 (Figure 6A). This JNK2-elicited stimulation was even more pronounced when γ-secretase derived from T20 cells that overexpress C99 was allowed to process C99 in the presence of active JNK2 (Figure 6B). In this experiment, the production of APP intracellular domain (AICD) resulting from γ-secretase–mediated processing of C99 and C83 was significantly increased in the presence of active JNK2. Addition of the γ-secretase inhibitor DAPT completely blocked the processing of C99 and C83, whereas control reactions in the absence of active JNK2 produced a modest amount of AICD (Figure 6C). These findings strongly support a model in which JNKs directly interact with and phosphorylate γ-secretase to augment its enzymatic activity.

A Putative Phosphorylation Site ($Ser^{319}Thr^{320}$) in PS1 Is Required for TNF-α–elicited Stimulation of γ-Secretase Activity

To elucidate the molecular mechanism underlying the JNK-dependent regulation of γ-secretase, it is necessary to identify the critical residues in NCT and PS1 that are subject to JNK-dependent phosphorylation. By using the algorithm provided by the NetPhos 2.0 Server (http://www.cbs.dtu.dk/services/NetPhos/; Blom *et al.*, 1999) to predict conserved Ser/Thr phosphorylation sites, we identified an adjacent Ser/Thr pair ($S^{319}T^{320}$) to be a likely candidate for phosphorylation by JNK. We thus hypothesized that a mutant PS1 lacking this putative phosphorylation site would be unresponsive to TNF-α–elicited stimulation. To test this hypothesis, we created a mutant PS1 (PS1-S319A/T320A) by simultaneously replacing the S^{319} and T^{320} residues in human PS1 with alanines using site-directed mutagenesis.

To examine whether the mutant PS1 could affect γ-secretase activity in response to TNF-α stimulation, γ-secretase activity in T20 cells transfected with either an empty vector, wild-type human PS1 (PS1-WT), or PS1-S319A/T320A was assessed in the presence or absence of TNF-α. As shown in Figure 7A, the increase in γ-secretase activity that is normally triggered by TNF-α was completely eradicated in cells expressing PS1-S319A/T320A, but not PS1-WT. Furthermore, these results revealed that cells expressing PS1-S319A/T320A exhibit similar levels of γ-secretase activity in the presence or absence of SP600125, consistent with the model that TNF-α–eclicited stimulation of γ-secretase is mediated by the JNK pathway. Our data suggest that $S^{319}T^{320}$ in PS1 is targeted by JNK in response to TNF-α–triggered regulation of γ-secretase.

Mutant PS1 (PS1-S319A/T320A) Can Prevent the TNF-α–stimulated Processing of NotchΔE by γ-Secretase

To ascertain whether JNK-dependent phosphorylation of PS1 can modulate the catalytic activity of γ-secretase inde-

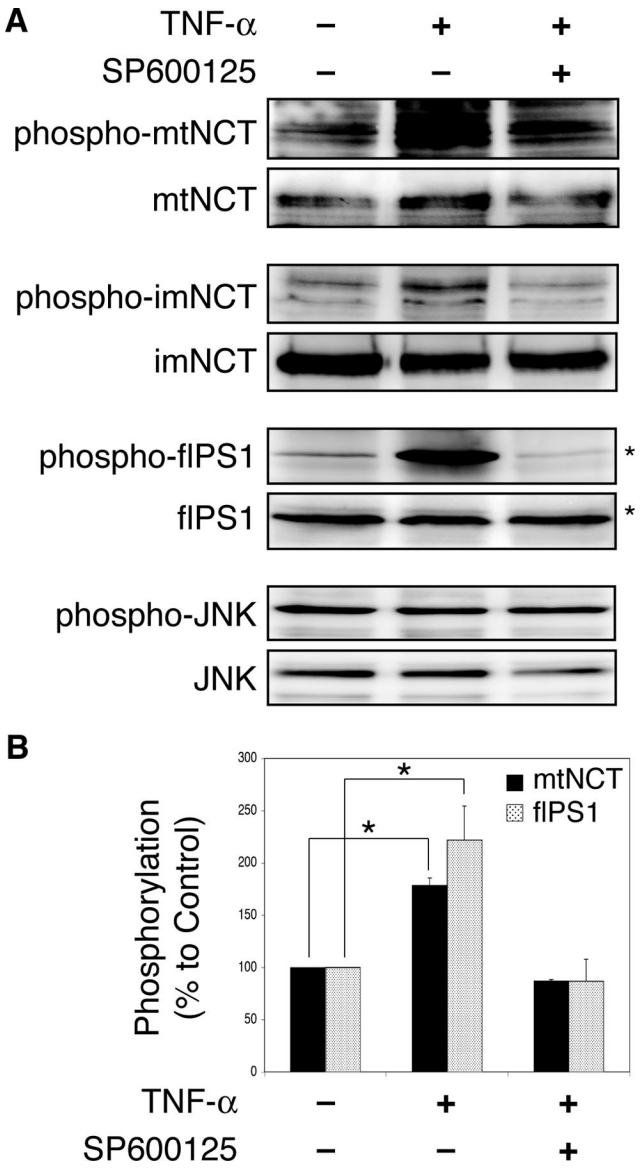

Figure 4. Suppression of TNF-α–induced phosphorylation of PS1 and NCT by a JNK inhibitor SP600125. (A) γNCT-36 cells (10^7 cells/plates) in 10-cm culture plates were preincubated with DMEM containing 0.5% FBS at 37°C for 3 h and were pretreated with vehicle alone (0.1% DMSO) or 10 μM SP600125, a JNK inhibitor, at 37°C for 30 min, followed by the addition of TNF-α to a final concentration of 20 ng/ml and an additional incubation at 37°C for 1.5 h. γ-Secretase complexes in cell lysates were purified by HIS-Selected Cobalt Affinity Gel through the affinity of the His-tagged NCT. Affinity-purified proteins were resolved by SDS-PAGE and analyzed by Western blotting. The phosphorylation levels of NCT and PS1 were visualized by an anti-phospho-serine/threonine antibody, whereas those of JNK by anti-phospho-JNK. The same blots were stripped and reprobed with anti-NCT, anti-PS1-NTF, and anti-total JNK antibodies to determine the levels of total NCT, PS1, and JNK. mtNCT, mature NCT; imNCT, immature NCT; flPS1, full-length PS1. Asterisk denotes the mobility shift of phosphorylated flPS1. (B) The levels of phosphorylated mtNCT and flPS1 were determined by densitometry and normalized by those of total mtNCT and flPS1, respectively. The normalized phosphorylation levels of mtNCT and flPS1 in untreated cells are referred to as 100% relative phosphorylation, respectively. Results are expressed as the mean (±SD) phosphorylation levels of mtNCT (solid bar) and flPS1 (hatched bar) from three independent experiments and analyzed by Student's *t* test. *$p < 0.05$.

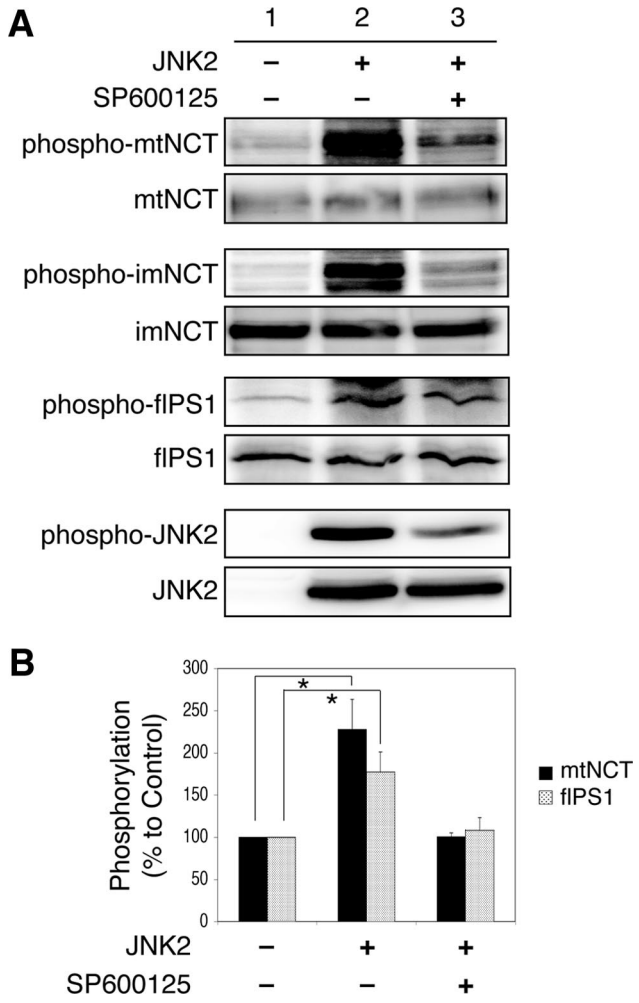

Figure 5. Active JNK2 can enhance the phosphorylation of NCT and PS1 in an in vitro kinase assay. (A) The microsomal membranes and solubilized γ-secretase of γNCT-36 cells were prepared as described in *Materials and Methods*. γ-Secretase was partially purified by HIS-Select Cobalt Affinity Gel through affinity of the His-tagged NCT. Affinity-purified γ-secretase (25 μg) was incubated with 200 ng active JNK2 at 30°C for 1 h in the presence (lane 3) or absence (lane 2) of 10 μM SP600125. A reaction containing only affinity-purified γ-secretase was included as a control (lane 1). The reaction mixtures were resolved by SDS-PAGE and analyzed by Western blotting with anti-phospho-serine/threonine, anti-phospho-JNK, anti-JNK, anti-NCT, and anti-PS1-NTF antibodies. (B) The levels of phosphorylated and total proteins were determined by densitometry. The ratio of phosphorylated versus total protein (NCT and flPS1) in the control reaction was referred to as 100% relative phosphorylation. Quantitative data are shown as the mean (±SD) phosphorylation of mtNCT and flPS1 from three independent experiments and analyzed by Student's *t* test. *$p < 0.05$.

pendent of substrate selectivity, N7 cells were transfected with an empty vector, PS1-WT, or PS1-S319A/T320A, followed by the treatments with TNF-α. We found that the TNF-α-stimulated processing of NotchΔE (NΔE) by γ-secretase in cells expressing mutant PS1-S319A/T320A is dramatically reduced, as evidenced by the decreased production of Notch intracellular domain (NICD), whereas endogenous γ-secretase cleavage of NΔE remains unaffected, as judged from comparison to the amount of NICD produced in cells transfected with PS1-WT (Figure 7, B and C). Consistent with its effect on γ-secretase cleavage of APP-C99 in T20 cells

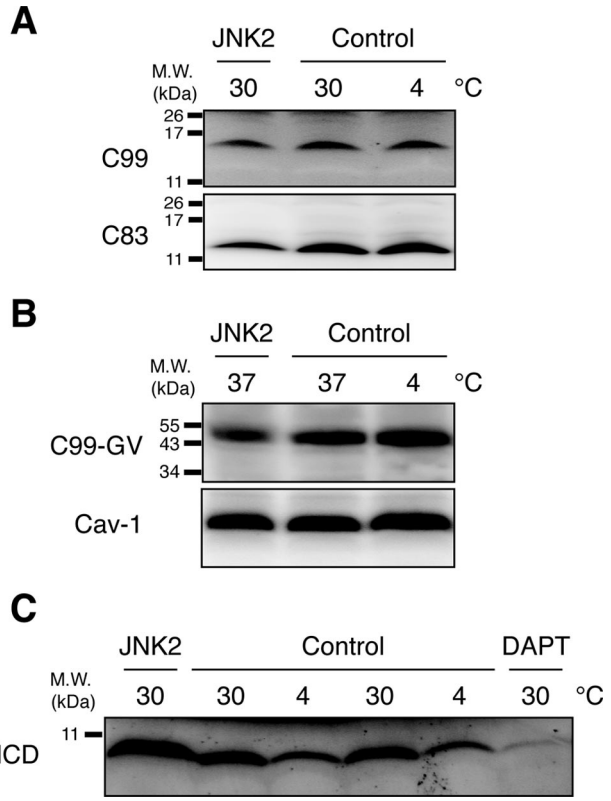

Figure 6. Active JNK2 promotes the processing of C99 and C83 to produce AICD. (A) Equivalent amounts of resuspended microsomal membranes that were derived from γNCT-36 cells and enriched with membrane-tethered γ-secretase and APP-CTFs was incubated with 200 ng active JNK2 and 200 μM ATP in a kinase buffer for 2 h at 30 or 4°C. Reactions lacking JNK2 were included as controls. Terminated reaction mixtures were resolved by tricine (16.5%) SDS-PAGE, and the levels of C99 and C83 were analyzed by Western blotting by using anti-Aβ1–17 (clone 6E10, for C99) and anti-APP C-terminus (C′APP, for C83) antibodies, respectively. (B) Equivalent amounts of resuspended microsomal membranes that were derived from T20 cells and enriched with membrane-tethered γ-secretase and C99-GV were incubated with 200 ng active JNK2 and 200 μM ATP in a kinase buffer for 4 h at 37 or 4°C. Reactions lacking JNK2 were included as controls. Terminated reaction mixtures were resolved by tricine (10%) SDS-PAGE, and the levels of C99 were analyzed by Western blotting by using anti-Aβ1–17 (clone 6E10). The levels of caveolin-1 were determined as a membrane protein loading control. (C) Equivalent amounts of resuspended microsomal membranes that were derived from γNCT-36 cells and enriched with membrane-tethered γ-secretase, and APP-CTFs were incubated with 200 ng active JNK2 and 200 μM ATP in a kinase buffer in the presence of 0.1% DMSO or 10 μM DATP for 2 h at 30 or 4°C. Reactions lacking JNK2 were included as controls. Terminated reaction mixtures were resolved by tricine (16.5%) SDS-PAGE, and the levels of AICD were analyzed by Western blotting by using an anti-APP C-terminus (C′APP) antibody. Molecular weight markers (MW, in kDa) are denoted to the left of each immunoblot.

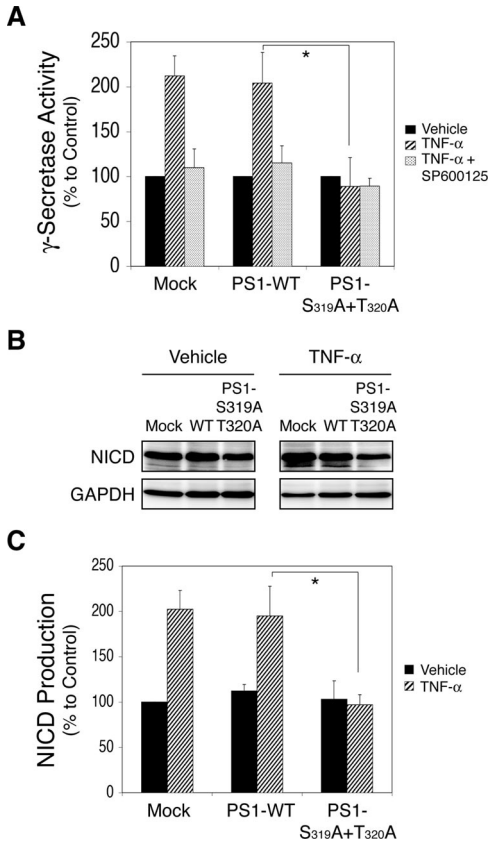

Figure 7. One putative phosphorylation site in human PS1, $S^{319}T^{320}$, is required for the TNF-α–elicited stimulation of γ-secretase activity. (A) T20 cells (7.5×10^5 cells/well) in six-well microplates were transfected with 1 μg/well of empty vector (Mock), wild-type PS1 (PS1-WT), or mutant PS1 (PS1-$S^{319}A+T^{320}A$) in the presence of 0.1 μg/well of pRL-TK for 24 h at 37°C, followed by replacing the media with DMEM containing 0.5% FBS and 1 μg/ml tetracycline in the presence of 0.1% DMSO (solid bar, striped bar) or 10 μM SP600125 (hatched bar) and an additional incubation at 37°C for at least 3 h. Transfected cells were then treated with 50 ng/ml TNF-α in DMEM containing 0.5% FBS at 37°C overnight (striped bar and hatched bar). γ-Secretase activity was determined by using the Dual-Glo luciferase assay reagents. Normalized luciferase signals from vehicle-treated cells were referred to as 100% relative γ-secretase activity. Data are shown as the mean (±SD) of triplicate measurements from three independent experiments and analyzed by Student's *t* test. *$p < 0.05$. (B) N7 cells (5×10^5 cells/well) in six-well tissue culture plates were transfected with 1 μg/well of empty vector (Mock), PS1-WT, or PS1-S319AT320A for 24 h at 37°C, followed by the replacement of medium with DMEM containing 0.5% FBS and an additional incubation for at least 3 h at 37°C. Transfected cells were treated with vehicle alone or 50 ng/ml TNF-α and incubated at 37°C overnight. Clarified lysates with equivalent amounts of proteins were resolved by SDS-PAGE and analyzed by Western blotting. The production of NICD was visualized by anti-Notch-(Val^{1744}) antibody (top panel). The levels of GAPDH were determined as a protein loading control (bottom panel). (C) The levels of NICD and GAPDH were determined by densitometry. The ratio of NICD versus GAPDH in untreated mock-transfected cells was referred to as 100% relative NICD production. Quantitative data are shown as the mean (±SD) NICD production from three independent experiments and analyzed by Student's *t* test. *$p < 0.05$.

(Figure 7A), these results suggest that ectopically expressed PS1-S319A/T320A can be processed and assembled into active γ-secretase complexes just as well as the wild-type PS1, as evidenced by the unchanged basal activity of endogenous γ-secretase. These findings substantiate that mutant PS1 defective in a JNK phosphorylation site can completely abolish the TNF-α–induced increase in γ-secretase activity independent of its available substrates. It is thus the deficiency in JNK phosphorylation of PS1 that attributes to the blockade of TNF-α–elicited effects on γ-secretase activity.

To further confirm that the S^{319} and T^{320} residues of PS1 are required for JNK phosphorylation, we generated one synthetic peptide (ST) encompassing the wild-type PS1 sequence flanking the $S^{319}T^{320}$ motif and another synthetic

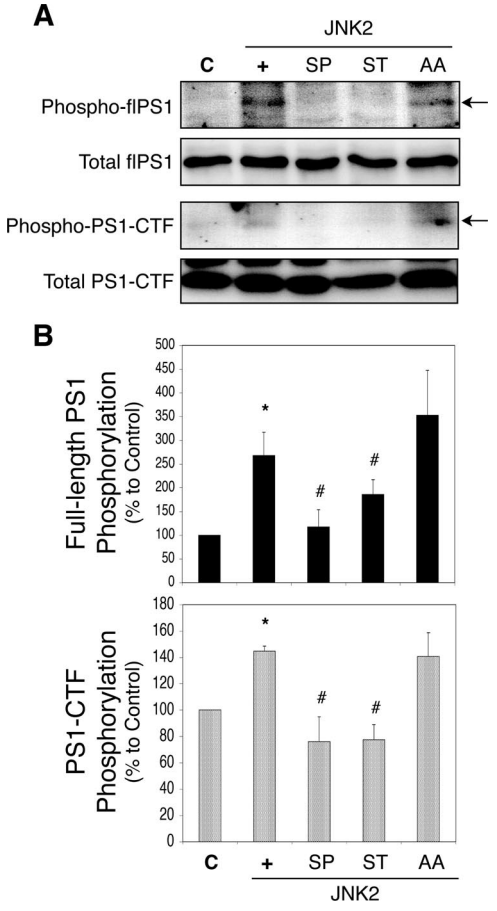

Figure 8. A synthetic peptide containing sequences flanking $S^{319}T^{320}$ effectively blocks JNK-mediated phosphorylation of PS1. (A) Equivalent amounts of solubilized γ-secretase derived from γNCT-36 cells were incubated with 200 ng active JNK2 and 200 μM ATP in a kinase buffer in the presence of SP600125 (SP, 100 μM), synthetic peptide ST (2 mM), or synthetic peptide AA (2 mM) for 1.5 h at 30 or 4°C. Reactions lacking JNK2 were included as negative controls (C), whereas those containing active JNK2 only as positive controls (+). Terminated reaction mixtures were resolved by SDS-PAGE, and the levels of phosphorylated full-length PS1 (flPS1), phosphorylated PS1-CTF, total flPS1, and total PS1-CTF were analyzed by Western blotting by using anti-phospho-serine/phospho-threonine (clone MPM-2, for phospho-flPS1 at top panel and phospho-PS1-CTF at lower middle panel), anti-PS1-NTF (for total flPS1, upper middle panel), and anti-PS1-loop (for total PS1-CTF, bottom panel) antibodies, respectively. Arrow denotes the phosphorylated flPS1 and PS1-CTF, respectively. (B) The levels of phosphorylated flPS1, phosphorylated PS1-CTF, total flPS1, and total PS1-CTF were determined by densitometry. The ratios of phospho-flPS1 versus total flPS1 (solid bar) and phospho-PS1-CTF versus total PS1-CTF (shaded bar) in control reactions lacking JNK2 was referred to as 100% relative phosphorylation of PS1 (histogram). Quantitative data are shown as the mean (±SD) PS1 phosphorylation from at least four independent experiments and analyzed by Student's *t* test. *$p < 0.05$ versus negative control (C). #$p < 0.05$ versus positive control (+).

peptide (AA) whose $S^{319}T^{320}$ residues are simultaneously replaced with alanines. Using both synthetic peptides as competitors in the in vitro JNK kinase assay, we found that JNK phosphorylation of PS1 (both full-length PS1 and PS1-CTF) is completely blocked by the wild-type synthetic peptide ST, but not by the mutant peptide AA, reminiscent of the inhibitory effect of SP600125 (Figure 8). Together, our data identify S^{319} and T^{320} in PS1 as an essential motif for JNK phosphorylation elicited by TNF-α signaling.

JNK-dependent Phosphorylation of PS1 Correlates with the Enhanced Stability of PS1-CTF

Given that the phosphorylation of full-length PS1 by JNK is important for its proteolytic activity and that the $S^{319}T^{320}$ phosphorylation site of PS1 is localized near an endoproteolytic site within the protein's intracellular hydrophilic loop domain, we hypothesized that JNK phosphorylation of PS1 might promote endoproteolysis of full-length PS1 to give an active heterodimer form of PS1, which is a prerequisite for the formation of functional γ-secretase complexes (Iwatsubo, 2004). Alternatively, JNK phosphorylation of PS1-$S^{319}T^{320}$ might simply prolong the stability of PS1-CTF. To determine whether the phosphorylation of PS1 by JNK influences the endoproteolysis of PS1 or the stability of PS1-CTF, we first examined the levels of full-length PS1, PS1-NTF, and PS1-CTF in response to JNK phosphorylation. The formation of PS1-NTF and PS1-CTF relative to the full-length PS1 in an in vitro kinase assay was assessed. We found that PS1 phosphorylation by an active recombinant JNK2 in a cell-free condition can significantly increase the levels of PS1-CTF relative to those of full-length PS1, whereas both the JNK inhibitor SP600125 and the wild-type synthetic peptide ST, but not the mutant peptide AA, can prevent the JNK-induced increase in the levels of PS1-CTF (Figure 9A). However, the levels of PS1-NTF relative to full-length PS1 in the same reactions were not significantly altered by JNK phosphorylation of PS1 (Figure 9B). Because JNK phosphorylation did not induce concomitant increases in the levels of PS1-CTF and PS1-NTF, these findings favor a model in which JNK phosphorylation of PS1 at $S^{319}T^{320}$ enhances the stability of phosphorylated PS1-CTF. Furthermore, we observed a significant increase in the ratio of PS1-CTF versus full-length PS1 in cells overexpressing wild-type PS1 (PS1-WT), but not mutant PS1 (PS1-S319A/T320A) that is defective in JNK phosphorylation (Figure 9C), suggesting that the stability of mutant PS1-CTF is significantly reduced. Our findings clearly demonstrate that JNK phosphorylation of PS1 at the $Ser^{319}Thr^{320}$ motif could be crucial for the stability of PS1-CTF in vivo, substantiating the biological significance of TNF-α–elicited JNK activation in the regulation of γ-secretase.

DISCUSSION

The generation of Aβ through the secretase-mediated processing of APP has long been thought to be causal for the neuropathology and cognitive decline in AD. Our previous study showed that activation of JNK is essential for the cytokine-elicited stimulation of γ-secretase activity (Liao *et al.*, 2004). Here, we provide new evidence demonstrating that TNF-α signaling can alter the phosphorylation status of PS1 and NCT, two major constituents of γ-secretase, concomitant with stimulation of γ-secretase activity. The newly established stable cell line γNCT-36 that stably overexpresses human wild-type PS1, NCT, Aph-1α, Pen-2, and APP provides a cellular model with unprecedented resolution of the posttranslational modifications to the components of γ-secretase in response to such extracellular stimuli as TNF-α. Using genetic and biochemical approaches, we clearly demonstrate that TNF-α–induced stimulation of γ-secretase is mediated through JNK phosphorylation of PS1 and NCT. We further identify a novel JNK phosphorylation site within human PS1 that is essential for both TNF-α–

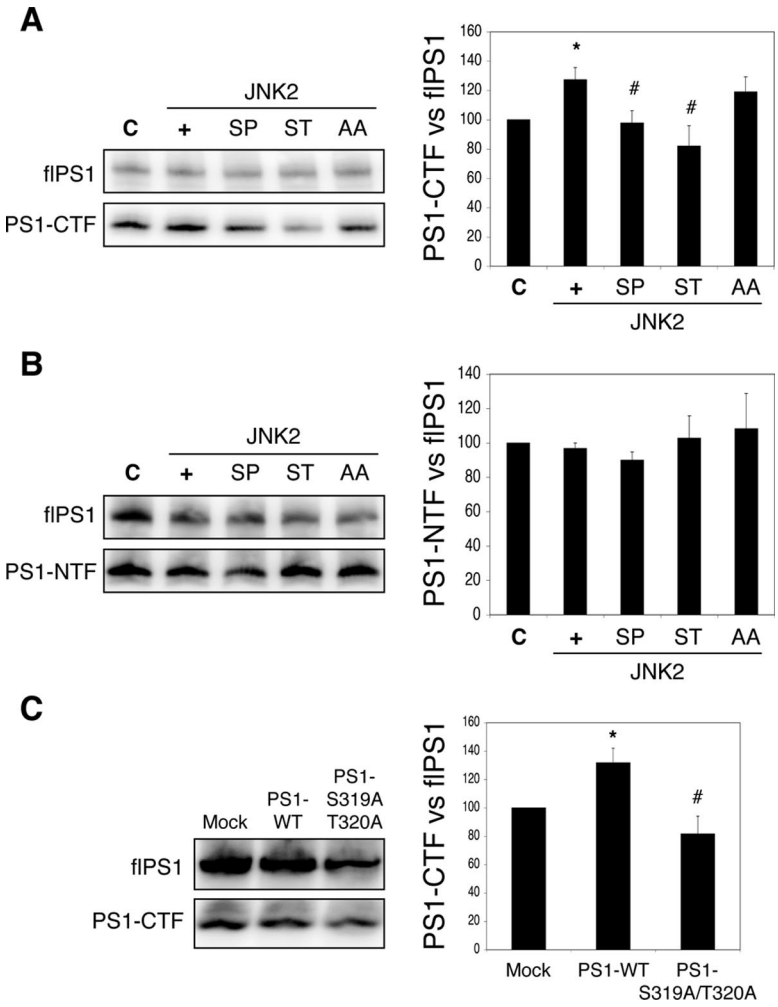

Figure 9. JNK phosphorylation of PS1 at $S^{319}T^{320}$ is essential for the stability of PS1-CTF. (A and B) Equivalent amounts of solubilized γ-secretase derived from γNCT-36 cells were incubated with 200 ng active JNK2 and 200 μM ATP in a kinase buffer in the presence of SP600125 (SP, 10 μM), synthetic peptide ST (2 mM), or synthetic peptide AA (2 mM) for 1 h at 30°C or 4°C. Reactions lacking JNK2 were included as negative controls (C), whereas those containing active JNK2 only as positive controls (+). Terminated reaction mixtures were resolved by SDS-PAGE and analyzed by Western blotting. The relative levels of PS1-CTF (bottom panel, A) versus full-length PS1 (flPS1, top panel, A) were visualized by using an anti-PS1-loop antibody (A), whereas those of PS1-NTF versus flPS1 by an anti-PS1-NTF antibody (B). The ratio of PS1-CTF versus flPS1 and that of PS1-NTF versus flPS1 in control reactions lacking JNK2 (C) were referred to as 100% relative levels of PS1 fragments (histogram). Quantitative data are shown as the mean (±SD) PS1-CTF levels (A) or PS1-NTF levels (B) from three independent experiments and analyzed by Student's *t* test. $^{*}p < 0.05$ versus negative control (C). $^{\#}p < 0.05$ versus positive control (+). (C) CHO cells (5×10^5 cells/well) in six-well microplates were transfected with 0.5 μg/well of empty vector (Mock), wild-type PS1 (PS1-WT), or mutant PS1 (PS1-$S^{319}A/T^{320}A$) for 24 h at 37°C. Transfected cells were solubilized by CHAPSO buffer, and clarified lysates containing equivalent amounts of protein were resolved by SDS-PAGE and analyzed by Western blotting with anti-PS1-loop to visualize full-length PS1 (flPS1, top panel) and PS1-CTF (bottom panel). The ratio of PS1-CTF versus flPS1 in mock-transfected cells was referred to as 100% relative levels of PS1-CTF (histogram). Quantitative data are shown as the mean (±SD) PS1-CTF levels from three independent experiments and analyzed by Student's *t* test. $^{*}p < 0.05$ versus Mock. $^{\#}p < 0.05$ versus PS1-WT.

induced stimulation of γ-secretase and the stability of PS1-CTF, correlating the JNK-dependent phosphorylation and the assembly of γ-secretase complexes.

Accumulated evidence reveals that JNKs play an important role in AD pathogenesis and that the application of JNK inhibitors could help alleviate the symptoms of AD (Manning and Davis, 2003; Zhu *et al.*, 2004b). Our data showing that down-regulation of JNKs by RNAi can dramatically attenuate both TNF-α–elicited and endogenous γ-secretase activity to reduce Aβ production (Figure 3), reminiscent of the inhibitory effect of the JNK-specific inhibitor SP600125, further support the neurodegenerative effects of JNKs on AD. Previous studies have demonstrated that down-regulation of JNK by RNAi can also effectively reduce the stress-induced phosphorylation of JNK (Nguyen *et al.*, 2005; Tong *et al.*, 2007), substantiating our data that the partial depletion of specific JNK isoforms could critically impair TNF-α–elicited regulation of γ-secretase. The JNK pathway is associated with age-dependent amyloid plaque deposition and the loss of synaptophysin in a Tg2576/PS1 double transgenic AD mouse model (Otth *et al.*, 2003). It is thus conceivable that all three major JNK isoforms (JNK1, JNK2, and JNK3) could be affected in AD (Shoji *et al.*, 2000; Ferrer *et al.*, 2001; Pei *et al.*, 2001; Zhu *et al.*, 2001). JNK1 and JNK2 exhibit a broad tissue distribution, whereas JNK3 is predominantly localized to pyramidal neurons in the CA1 and CA2 regions of the hippocampus, the neocortex, and the testes (Kuan *et al.*, 1999). Given that different JNK isoforms could have distinct biological functions (Davis, 2000), it is possible that they might not all participate to the same extent in mediating TNF-α–elicited regulation of γ-secretase. Recent studies have demonstrated that JNK2 and JNK3 are the primary mediators of MPTP-induced death of dopaminergic neurons, implicating a JNK-dependent neurodegeneration in the pathogenesis of Parkinson's disease (Hunot *et al.*, 2004). In addition, JNK3 has also been implicated as the principal mediator of ischemia-hypoxia–associated neuronal death (Kuan *et al.*, 2003). Although JNK1/2/3 are all involved in the regulation of both endogenous and TNF-α–elicited γ-secretase activity, our data suggest that JNK1/2 are the primary mediators of TNF-α's stimulatory effects, further substantiating the idea that individual JNK isoforms could have distinct roles in a variety of biological functions.

Our present data provide evidence for the first time that JNKs can directly interact with γ-secretase (Figure 5), further strengthening the importance of the JNK pathway in the regulation of APP processing. In cultured γNCT-36 cells, JNK can also be coprecipitated with NCT, PS1, and the full-length APP (data not shown), which can be suppressed by the inhibition of JNK, suggesting that phosphorylation of γ-secretase by JNK could affect the interactions between this protease and its substrates. Given that JNK can also phosphorylate APP at Thr^{668} (Standen *et al.*, 2001), our results clearly suggest that γ-secretase could physically interact

with APP and JNK. Because Aβ-induced activation of JNK plays a critical role in Aβ-dependent neuronal death in AD (Morishima *et al.*, 2001), it is likely that phosphorylation of APP and γ-secretase by JNK could synergistically promote the processing of APP through simultaneously turning APP into a favorable substrate (phosphorylated APP) and elevating γ-secretase activity, constituting a positive feedback to potentiate the Aβ-elicited neurotoxicity.

We identify a novel JNK phosphorylation site within PS1 at Ser^{319} and Thr^{320} that is susceptible to TNF-α signaling. Ser^{319} and Thr^{320} are located within the nonconserved hydrophilic loop domain of PS1 that encompasses additional phosphorylation sites, including Ser^{310}, Ser^{346}, Ser^{353}, Ser^{354}, and Ser^{357}, utilized by such intracellular kinases as PKA, PKC, GSK-3β, and CDK5 (Kirschenbaum *et al.*, 2001b; Lau *et al.*, 2002; Fluhrer *et al.*, 2004). Despite the marginal effect of phosphorylation of PS1 by PKC on Aβ production (Seeger *et al.*, 1997; Walter *et al.*, 1997), phosphorylation of PS1 by various kinases at distinct residues has been shown to affect the binding of PS1 to β-catenin and its nuclear signaling, PS1-CTF protein stability, and the caspase cleavage of PS1 (Kirschenbaum *et al.*, 2001a; Lau *et al.*, 2002; Fluhrer *et al.*, 2004; Prager *et al.*, 2007). Consistent with previous findings, our present data, that modulation of γ-secretase activity is susceptible to TNF-α–elicited JNK phosphorylation of PS1 at $Ser^{319}Thr^{320}$, suggest that the processing, stability, and function of PS1 are regulated in a complex manner.

We present evidence that the deficiency in JNK phosphorylation of PS1 at $S^{319}T^{320}$ could result in reduced levels of PS1-CTF, but not PS1-NTF, implying that the stability of PS1 heterodimers could be subject to the regulation elicited by extracellular stimuli. This finding is in accordance with the observation that the stabilities of the individual PS1 fragments appear to be regulated independently (Kirschenbaum *et al.*, 2001a). Of note, cells expressing the PS1-S319A/T320A mutant exhibit consistent endoproteolysis of PS1 and have normal basal γ-secretase activity just like those expressing wild-type PS1 do. The processing of full-length PS1 into PS1-NTF and PS1-CTF fragments is a prerequisite for the formation of stable heterodimers that are incorporated into high molecular mass complexes (Iwatsubo, 2004). Although the nonconserved hydrophilic loop domain of PS1 has been shown to be dispensable for PS1 endoproteolysis (Saura *et al.*, 2000), recent evidence demonstrates that phosphorylation of this domain by GSK-3β could induce a structural change in PS1 (Prager *et al.*, 2007). Accordingly, phosphorylation of the hydrophilic loop domain by JNK might also induce a conformational change in PS1-CTF, augmenting its stability. It is thus plausible that phosphorylated PS1-CTF could effectively interact with PS1-NTF to form PS1-NTF/CTF heterodimers and render γ-secretase complexes with higher catalytic activities. Alternatively, phosphorylation of PS1 by JNK could affect its interaction with other intracellular signaling modulators that in turn control γ-secretase activity. Both scenarios highlight the functional role of TNF-α–elicited phosphorylation of PS1 and NCT by JNK in the regulation of γ-secretase.

Together, our results demonstrate that TNF-α–elicited activation of γ-secretase is due to the JNK-dependent phosphorylation of PS1 and NCT, possibly through a direct interaction between JNK and γ-secretase. Our data also propose that $S^{319}T^{320}$ is the major JNK phosphorylation site in PS1. The exact role of JNK phosphorylation of PS1 and NCT and how such events can affect the protein–protein interactions among various γ-secretase constituents warrants further investigation. Finally, molecules able to block phosphorylation of PS1 by JNK might inhibit the γ-secretase–mediated processing of APP and possibly provide the basis for the development of novel anti-AD drugs.

ACKNOWLEDGMENTS

We thank Dr. Michael Wolfe for providing γ-30 cells and human PS1 and NCT cDNA constructs. We are grateful to Drs. Jen-Leih Wu, John Yu, and to Nin-Nin Chuang for generous support. The authors thank the Core Facility of the Institute of Cellular and Organismic Biology, Academia Sinica for technical support. DNA sequencing analyses were carried out by the Core Facilities for Basic Genomic Research located at the National Yang-Ming University Genome Center. This study was supported by the National Science Council, Taiwan, Grants NSC 93-2320-B-001-037, NSC 94-2320-B-001-004, NSC 94-3112-B-001-001, NSC 95-3112-B-001-006, and NSC 95-2320-B-001-041-MY2 (Y.-F. L.) and Academia Sinica (Y.-F.L.).

REFERENCES

Bakshi, P., Liao, Y. F., Gao, J., Ni, J., Stein, R., Yeh, L. A., and Wolfe, M. S. (2005). A high-throughput screen to identify inhibitors of amyloid β-protein precursor processing. J. Biomol. Screen. *10*, 1–12.

Bamberger, M. E., Harris, M. E., McDonald, D. R., Husemann, J., and Landreth, G. E. (2003). A cell surface receptor complex for fibrillar beta-amyloid mediates microglial activation. J. Neurosci. *23*, 2665–2674.

Bentahir, M., Nyabi, O., Verhamme, J., Tolia, A., Horre, K., Wiltfang, J., Esselmann, H., and De Strooper, B. (2006). Presenilin clinical mutations can affect gamma-secretase activity by different mechanisms. J. Neurochem. *96*, 732–742.

Blom, N., Gammeltoft, S., and Brunak, S. (1999). Sequence and structure-based prediction of eukaryotic protein phosphorylation sites. J. Mol. Biol. *294*, 1351–1362.

Combs, C. K., Karlo, J. C., Kao, S. C., and Landreth, G. E. (2001). β-Amyloid stimulation of microglia and monocytes results in TNFα-dependent expression of inducible nitric oxide synthase and neuronal apoptosis. J. Neurosci. *21*, 1179–1188.

Davis, R. J. (2000). Signal transduction by the JNK group of MAP kinases. Cell *103*, 239–252.

De Strooper, B. (2007). Loss-of-function presenilin mutations in Alzheimer disease. Talking Point on the role of presenilin mutations in Alzheimer disease. EMBO Rep. *8*, 141–146.

Esler, W. P., Kimberly, W. T., Ostaszewski, B. L., Ye, W., Diehl, T. S., Selkoe, D. J., and Wolfe, M. S. (2002). Activity-dependent isolation of the presenilin–γ-secretase complex reveals nicastrin and a gamma substrate. Proc. Natl. Acad Sci. USA *99*, 2720–2725.

Esler, W. P., and Wolfe, M. S. (2001). A portrait of Alzheimer secretases—new features and familiar faces. Science *293*, 1449–1454.

Ferrer, I., Blanco, R., Carmona, M., and Puig, B. (2001). Phosphorylated mitogen-activated protein kinase (MAPK/ERK-P), protein kinase of 38 kDa (p38-P), stress-activated protein kinase (SAPK/JNK-P), and calcium/calmodulin-dependent kinase II (CaM kinase II) are differentially expressed in tau deposits in neurons and glial cells in tauopathies. J. Neural Transm. *108*, 1397–1415.

Fluhrer, R., Friedlein, A., Haass, C., and Walter, J. (2004). Phosphorylation of presenilin 1 at the caspase recognition site regulates its proteolytic processing and the progression of apoptosis. J. Biol. Chem. *279*, 1585–1593.

Fraering, P. C., Ye, W., Strub, J. M., Dolios, G., LaVoie, M. J., Ostaszewski, B. L., van Dorsselaer, A., Wang, R., Selkoe, D. J., and Wolfe, M. S. (2004). Purification and characterization of the human gamma-secretase complex. Biochemistry *43*, 9774–9789.

Hunot, S., Vila, M., Teismann, P., Davis, R. J., Hirsch, E. C., Przedborski, S., Rakic, P., and Flavell, R. A. (2004). JNK-mediated induction of cyclooxygenase 2 is required for neurodegeneration in a mouse model of Parkinson's disease. Proc. Natl. Acad. Sci. USA *101*, 665–670.

Iwatsubo, T. (2004). The gamma-secretase complex: machinery for intramembrane proteolysis. Curr. Opin. Neurobiol. *14*, 379–383.

Katagiri, C., Negishi, K., and Hibino, T. (2006). c-JUN N-terminal kinase-1 (JNK1) but not JNK2 or JNK3 is involved in UV signal transduction in human epidermis. J. Dermatol. Sci. *43*, 171–179.

Kimberly, W. T., LaVoie, M. J., Ostaszewski, B. L., Ye, W., Wolfe, M. S., and Selkoe, D. J. (2003). Gamma-secretase is a membrane protein complex comprised of presenilin, nicastrin, Aph-1, and Pen-2. Proc. Natl. Acad. Sci. USA *100*, 6382–6387.

Kimberly, W. T., and Wolfe, M. S. (2003). Identity and function of gamma-secretase. J. Neurosci. Res. *74*, 353–360.

Kirschenbaum, F., Hsu, S. C., Cordell, B., and McCarthy, J. V. (2001a). Glycogen synthase kinase-3beta regulates presenilin 1 C-terminal fragment levels. J. Biol. Chem. *276*, 30701–30707.

Kirschenbaum, F., Hsu, S. C., Cordell, B., and McCarthy, J. V. (2001b). Substitution of a glycogen synthase kinase-3beta phosphorylation site in presenilin 1 separates presenilin function from beta-catenin signaling. J. Biol. Chem. *276*, 7366–7375.

Kuan, C. Y., *et al.* (2003). A critical role of neural-specific JNK3 for ischemic apoptosis. Proc. Natl. Acad. Sci. USA *100*, 15184–15189.

Kuan, C. Y., Yang, D. D., Samanta Roy, D. R., Davis, R. J., Rakic, P., and Flavell, R. A. (1999). The Jnk1 and Jnk2 protein kinases are required for regional specific apoptosis during early brain development. Neuron *22*, 667–676.

Lau, K. F., Howlett, D. R., Kesavapany, S., Standen, C. L., Dingwall, C., McLoughlin, D. M., and Miller, C. C. (2002). Cyclin-dependent kinase-5/p35 phosphorylates presenilin 1 to regulate carboxy-terminal fragment stability. Mol. Cell. Neurosci. *20*, 13–20.

Lee, H. G., Casadesus, G., Zhu, X., Takeda, A., Perry, G., and Smith, M. A. (2004). Challenging the amyloid cascade hypothesis: senile plaques and amyloid-beta as protective adaptations to Alzheimer disease. Ann. NY Acad. Sci. *1019*, 1–4.

Lee, H. G., Zhu, X., Nunomura, A., Perry, G., and Smith, M. A. (2006). Amyloid beta: the alternate hypothesis. Curr. Alzheimer Res. *3*, 75–80.

Liao, Y. F., Wang, B. J., Cheng, H. T., Kuo, L. H., and Wolfe, M. S. (2004). Tumor necrosis factor-alpha, interleukin-1beta, and interferon-gamma stimulate gamma-secretase-mediated cleavage of amyloid precursor protein through a JNK-dependent MAPK pathway. J. Biol. Chem. *279*, 49523–49532.

Liao, Y. F., Wang, B. J., Hsu, W. M., Lee, H., Liao, C. Y., Wu, S. Y., Cheng, H. T., and Hu, M. K. (2007). Unnatural amino acid-substituted (hydroxyethyl)urea peptidomimetics inhibit gamma-secretase and promote the neuronal differentiation of neuroblastoma cells. Mol. Pharmacol. *71*, 588–601.

Manning, A. M., and Davis, R. J. (2003). Targeting JNK for therapeutic benefit: from junk to gold? Nat. Rev. Drug Discov. *2*, 554–565.

McLendon, C. *et al.* (2000). Cell-free assays for gamma-secretase activity. FASEB J. *14*, 2383–2386.

Morishima, Y., Gotoh, Y., Zieg, J., Barrett, T., Takano, H., Flavell, R., Davis, R. J., Shirasaki, Y., and Greenberg, M. E. (2001). Beta-amyloid induces neuronal apoptosis via a mechanism that involves the c-Jun N-terminal kinase pathway and the induction of Fas ligand. J. Neurosci. *21*, 7551–7560.

Nguyen, M. T., Satoh, H., Favelyukis, S., Babendure, J. L., Imamura, T., Sbodio, J. I., Zalevsky, J., Dahiyat, B. I., Chi, N. W., and Olefsky, J. M. (2005). JNK and tumor necrosis factor-alpha mediate free fatty acid-induced insulin resistance in 3T3–L1 adipocytes. J. Biol. Chem. *280*, 35361–35371.

Otth, C., Mendoza-Naranjo, A., Mujica, L., Zambrano, A., Concha, I. I., and Maccioni, R. B. (2003). Modulation of the JNK and p38 pathways by cdk5 protein kinase in a transgenic mouse model of Alzheimer's disease. Neuroreport *14*, 2403–2409.

Pei, J. J., Braak, E., Braak, H., Grundke-Iqbal, I., Iqbal, K., Winblad, B., and Cowburn, R. F. (2001). Localization of active forms of C-jun kinase (JNK) and p38 kinase in Alzheimer's disease brains at different stages of neurofibrillary degeneration. J. Alzheimers Dis. *3*, 41–48.

Prager, K., Wang-Eckhardt, L., Fluhrer, R., Killick, R., Barth, E., Hampel, H., Haass, C., and Walter, J. (2007). A structural switch of presenilin 1 by glycogen synthase kinase 3beta-mediated phosphorylation regulates the interaction with beta-catenin and its nuclear signaling. J. Biol. Chem. *282*, 14083–14093.

Qin, W., Ho, L., Pompl, P. N., Peng, Y., Zhao, Z., Xiang, Z., Robakis, N. K., Shioi, J., Suh, J., and Pasinetti, G. M. (2003). Cyclooxygenase (COX)-2 and COX-1 potentiate beta-amyloid peptide generation through mechanisms that involve gamma-secretase activity. J. Biol. Chem. *278*, 50970–50977.

Reynolds, C. H., Betts, J. C., Blackstock, W. P., Nebreda, A. R., and Anderton, B. H. (2000). Phosphorylation sites on tau identified by nanoelectrospray mass spectrometry: differences in vitro between the mitogen-activated protein kinases ERK2, c-Jun N-terminal kinase and P38, and glycogen synthase kinase-3beta. J. Neurochem. *74*, 1587–1595.

Saura, C. A., Tomita, T., Soriano, S., Takahashi, M., Leem, J. Y., Honda, T., Koo, E. H., Iwatsubo, T., and Thinakaran, G. (2000). The nonconserved hydrophilic loop domain of presenilin (PS) is not required for PS endoproteolysis or enhanced abeta 42 production mediated by familial early onset Alzheimer's disease-linked PS variants. J. Biol. Chem. *275*, 17136–17142.

Seeger, M. *et al.* (1997). Evidence for phosphorylation and oligomeric assembly of presenilin 1. Proc. Natl. Acad. Sci. USA *94*, 5090–5094.

Selkoe, D. J. (2001). Alzheimer's disease: genes, proteins, and therapy. Physiol. Rev. *81*, 741–766.

Shoji, M., Iwakami, N., Takeuchi, S., Waragai, M., Suzuki, M., Kanazawa, I., Lippa, C. F., Ono, S., and Okazawa, H. (2000). JNK activation is associated with intracellular beta-amyloid accumulation. Brain Res. Mol. Brain Res. *85*, 221–233.

Standen, C. L., Brownlees, J., Grierson, A. J., Kesavapany, S., Lau, K. F., McLoughlin, D. M., and Miller, C. C. (2001). Phosphorylation of thr(668) in the cytoplasmic domain of the Alzheimer's disease amyloid precursor protein by stress-activated protein kinase 1b (Jun N-terminal kinase-3). J. Neurochem. *76*, 316–320.

Tanzi, R. E., and Bertram, L. (2005). Twenty years of the Alzheimer's disease amyloid hypothesis: a genetic perspective. Cell *120*, 545–555.

Tong, C., Yin, Z., Song, Z., Dockendorff, A., Huang, C., Mariadason, J., Flavell, R. A., Davis, R. J., Augenlicht, L. H., and Yang, W. (2007). c-Jun NH2-terminal kinase 1 plays a critical role in intestinal homeostasis and tumor suppression. Am. J. Pathol. *171*, 297–303.

Vingtdeux, V., *et al.* (2005). Phosphorylation of amyloid precursor carboxy-terminal fragments enhances their processing by a gamma-secretase-dependent mechanism. Neurobiol. Dis. *20*, 625–637.

Walter, J., *et al.* (1997). Proteolytic processing of the Alzheimer disease-associated presenilin-1 generates an in vivo substrate for protein kinase C. Proc. Natl. Acad. Sci. USA *94*, 5349–5354.

Weggen, S., Eriksen, J. L., Sagi, S. A., Pietrzik, C. U., Golde, T. E., and Koo, E. H. (2003). Abeta42-lowering nonsteroidal anti-inflammatory drugs preserve intramembrane cleavage of the amyloid precursor protein (APP) and ErbB-4 receptor and signaling through the APP intracellular domain. J. Biol. Chem. *278*, 30748–30754.

Wei, Y., Yu, L., Bowen, J., Gorovsky, M. A., and Allis, C. D. (1999). Phosphorylation of histone H3 is required for proper chromosome condensation and segregation. Cell *97*, 99–109.

Wolfe, M. S. (2007). When loss is gain: reduced presenilin proteolytic function leads to increased Abeta42/Abeta40. Talking Point on the role of presenilin mutations in Alzheimer disease. EMBO Rep. *8*, 136–140.

Zhu, X., Raina, A. K., Lee, H. G., Casadesus, G., Smith, M. A., and Perry, G. (2004a). Oxidative stress signalling in Alzheimer's disease. Brain Res. *1000*, 32–39.

Zhu, X., Raina, A. K., Perry, G., and Smith, M. A. (2004b). Alzheimer's disease: the two-hit hypothesis. Lancet Neurol. *3*, 219–226.

Zhu, X., Raina, A. K., Rottkamp, C. A., Aliev, G., Perry, G., Boux, H., and Smith, M. A. (2001). Activation and redistribution of c-jun N-terminal kinase/stress activated protein kinase in degenerating neurons in Alzheimer's disease. J. Neurochem. *76*, 435–441.